Analysis of resonances of the imperfect acoustic cloaking*

KIM Seungil†

Department of Mathematics and Research Institute for Basic Sciences, Kyung Hee University, Seoul 130-701, Korea

(Received 20 August 2012)

In this paper, we study the resonance phenomenon arising from the imperfect acoustic cloaking in 2D based on a small perturbation of the transformation acoustics. We show that resonance frequencies of the imperfect cloaking appearing in the total scattering cross section converge to Dirichlet eigenvalues of the concealed region as a perturbation parameter approaches zero. This theory enables us to predict the location of resonance frequencies of the imperfect cloaking and identify the corresponding resonance modes.

PACS numbers: 43.20.Bi, 43.20.Fn, 43.20.+g

Recently, a transformation-based cloaking technique [1–3] has attracted enormous attention in many areas such as physics, mathematics and engineerings. The basic idea of the cloaking technique based on a transformation is to control wave fields in such a way that they bend smoothly around objects to be concealed and return to the original trajectory without producing any scattered fields. So the objects in the concealed region can be made invisible from detectors outside of the cloaking devices. This promising technology has been applied to various wave fields including electrostatics [1, 2], acoustics [4–9], electromagnetics [3, 10] and quantum fields [11].

A transformation proposed for the cloaking in $\mathbb{R}^2$ is obtained by compressing a punctured disc $B_b \setminus \{0\}$ of radius b radially to a concentric cylindrical shell $B_b \setminus \bar{B}_a$ bounded by circles of radii a and b, Γ_a and Γ_b, respectively, with $0 < a < b$. Mathematically, the compression is introduced by a singular transformation [11, 12]

$$F(x) = \left(\frac{b-a}{b}|x| + a\right)\frac{x}{|x|} \quad \text{for } 0 < |x| < b, \tag{1}$$

which blows up the center of B_b to the circle Γ_a. Then the acoustic pressure u satisfies the generalized Helmholtz equation

$$K\nabla \cdot \rho^{-1}\nabla u + k^2 u = 0 \quad \text{in } B_b \setminus \bar{B}_a, \tag{2}$$

where k is the wavenumber in the host medium, K and ρ represent bulk modulus and mass density tensor of the cloaking material, respectively. They are the material parameters induced by bringing the trivial material properties of B_b into $B_b \setminus \bar{B}_a$ via the transformation F. They are given by

$$\rho_r = r/(r-a), \tag{3}$$

$$\rho_\theta = (r-a)/r, \tag{4}$$

$$K = ((b-a)/b)^2 \times r/(r-a) \tag{5}$$

in cylindrical coordinates [5, 9].

Because of the singularity of the material parameters in the cloaking layer (a component of the mass density tensor is infinity on the inner boundary of the cloaking layer), it is challenging or impossible to fabricate the desired material in practice. To avoid the singular nature of the ideal cloaking scheme, an approximate cloaking technique has been proposed by using a small perturbation of the singular transformation, which maps the cylindrical layer $B_b \setminus \bar{B}_\varepsilon$ to $B_b \setminus \bar{B}_a$ with $\varepsilon > 0$ much smaller than the wave length of probing waves [18].

To quantify the effect of the approximate cloaking for various perturbation parameters and wavenumbers, the total scattering cross section (TSCS) has been investigated [13, 14]. The TSCS is obtained by integrating the far-field amplitude over all azimuthal angles and represents the total scattered power when the incident field is a plane wave with the unit amplitude. In Ref. [15, 16], the TSCS is also importantly utilized for measurement of the efficiency of the multi-layered realization [8, 17] of the ideal cloaking. In the references mentioned above, resonance phenomena are observed in the TSCS spectrum of the cloaking devices with air placed in the cloaked region. As resonances are one of major sources of noises, it is crucial to understand their origin and be able to predict their location in the TSCS spectrum in designing cloaking devices. Understanding distribution of wave fields of resonance frequencies in the concealed region is also of importance in developing an application such as sound insulation based on the cloaking scheme. In Ref. [13] it is realized that the resonance phenomenon is an inherent character of the cloaking devices when concealing penetrable media by investigating the scattering coefficients of scattered fields. However, the identification of resonance frequencies and the shape of corresponding resonance modes has not been clarified yet. In this paper, we analyze resonance frequencies of the imperfect cloaking based on a perturbed transformation and identify the shape of corresponding resonance modes. More precisely, we theoretically show that resonance phenomena of the imperfect cloaking arise near Dirichlet eigenvalues of the concealed region.

We first investigate the total scattering cross section (TSCS) of the approximate cloaking in $\mathbb{R}^2$ based on a

* This work was supported by a grant from the Kyung Hee University in 2012. (KHU-20120491)

† Electronic mail: sikim@khu.ac.kr

small perturbation of the transformation acoustics [18]. Assume that a plane incident field u^{in} with an amplitude p_0 is propagating along the x-direction:

$$u^{in} = p_0 e^{ikx} = p_0 \sum_{n=-\infty}^{\infty} i^n J_n(kr) e^{in\theta} \tag{6}$$

in cylindrical coordinates (r, θ). Let $f_\varepsilon(r) = (b-\varepsilon)(r-b)/(b-a)+b$ for $a < r < b$ be the inverse function of the radial function involved in the perturbed transformation [18]. Then the scattered fields u^{sc} outside of the cloaking structure, the fields u^{sh} in the cloaking shell and transmitted fields u^{tr} into the cloaked region can be written as

$$\begin{cases} u^{tr} = p_0 \displaystyle\sum_{n=-\infty}^{\infty} a_n J_n(kr) e^{in\theta} \quad \text{for } r < a, \\ u^{sh} = p_0 \displaystyle\sum_{n=-\infty}^{\infty} (i^n J_n(k f_\varepsilon(r)) + b_n H_n^1(k f_\varepsilon(r))) e^{in\theta} \\ \qquad\qquad\qquad\qquad\qquad \text{for } a < r < b, \\ u^{sc} = p_0 \displaystyle\sum_{n=-\infty}^{\infty} b_n H_n^1(kr) e^{in\theta} \quad \text{for } r > b, \end{cases} \tag{7}$$

where J_n is the Bessel function of order n and H_n^1 is the Hankel function of order n and of the first kind. Here the coefficients a_n and b_n are constants to be determined by the continuity of pressure fields and normal flux on the interface, $r = a$, between the cloaked region and the cloaking layer, that is, a_n and b_n are solutions to the system of equations

$$\begin{bmatrix} -\varepsilon (H_n^1)'(k\varepsilon) & a J_n'(ka) \\ -H_n^1(k\varepsilon) & J_n(ka) \end{bmatrix} \begin{bmatrix} a_n \\ b_n \end{bmatrix} = i^n \begin{bmatrix} \varepsilon J_n'(k\varepsilon) \\ J_n(k\varepsilon) \end{bmatrix}. \tag{8}$$

A simple computation yields that

$$a_n = -2i^n/(\pi k d_{n,\varepsilon}), \tag{9}$$
$$b_n = -i^n (a J_n'(ka) J_n(k\varepsilon) - \varepsilon J_n'(k\varepsilon) J_n(ka))/d_{n,\varepsilon}, \tag{10}$$

where $d_{n,\varepsilon}$ is the determinant of the matrix

$$d_{n,\varepsilon} = a J_n'(ka) H_n^1(k\varepsilon) - \varepsilon (H_n^1)'(k\varepsilon) J_n(ka). \tag{11}$$

Now, the TSCS is given by integration of the far-field amplitude and can be represented by the series in terms of scattering coefficients,

$$\text{TSCS} = \frac{4}{k} \sum_{n=-\infty}^{\infty} |b_n|^2. \tag{12}$$

The graphs of TSCS for $\varepsilon = 0.1, 0.01$ and 0.001 up to $ka = 11$ are given in Fig. 1, from which it is observed that many resonance peaks or dips occur in the TSCS spectrum. Clearly, the TSCS gets smaller as ε approaches zero except for resonance frequencies, as expected from the theoretical analysis [12]. Another observation is that there are quite narrow resonance peaks, N21, N22, N31

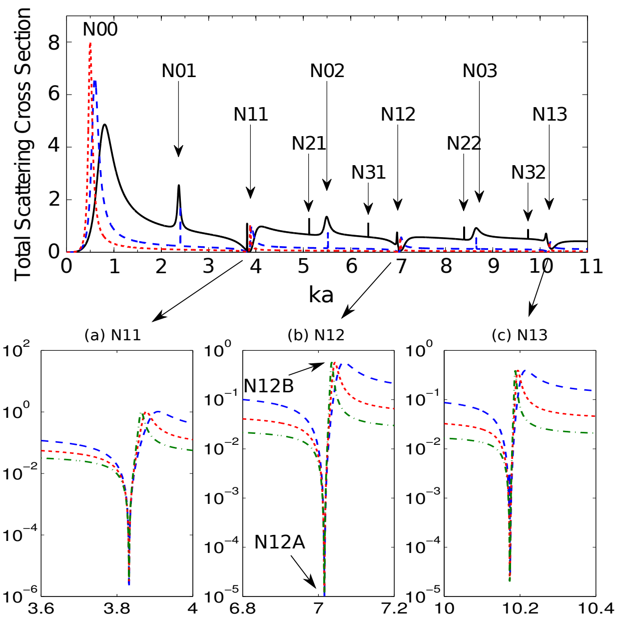

FIG. 1. Graph of TSCS. The solid, dashed, dotted (and dash-dotted in the bottom) curves correspond to the graphs of the TSCS for $\varepsilon = 0.1, 0.01$, 0.001 (and 0.0001) respectively.

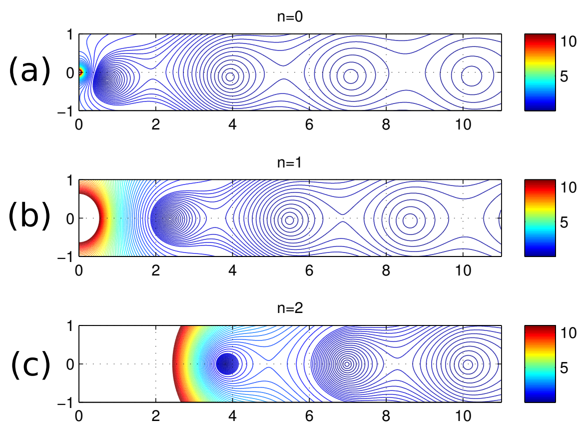

FIG. 2. Contour plots of $|d_{n,\varepsilon}(\lambda)|$ on the λ-plane for $a = 1$, $\varepsilon = 0.1$ and $n = 0, 1, 2$. The zeros of $d_{n,\varepsilon}(\lambda) = 0$ can be estimated by examining centers of the concentric circles of coutour plots.

and N32 of the black solid curve and N01, N02 and N03 of the blue dashed curve. It is found that higher resolution near some of the narrow resonance peaks is required for the presentation of the plot, which shows that resonances from the cloaking structure is extremely sensitive to wavenumbers for small ε.

Our goal is to understand how resonance frequencies behave as a function of the perturbation parameter ε and to predict the location of resonance frequencies. The resonance frequency k is thought of as the real part of a complex resonance eigenvalue λ, for which the cloaking system has a non-zero solution, that is, $k = \Re(\lambda)$ is a resonance frequency if and only if $d_{n,\varepsilon}(\lambda) = 0$. Fig. 2 exhibits the contour plots of the function $|d_{n,\varepsilon}(\lambda)|$ on the λ-plane for $\varepsilon = 0.1$ and $n = 0, 1, 2$ when $a = 1$, which allows us to estimate the location of complex resonance eigenvalues. Here, we recall that Dirichlet eigenvalues of the concealed unit disc are given by zeros of J_n. The plot in Fig. 2(b) displays the contours when $n = 1$, from which it can be deduced that zeros of the equation $d_1(\lambda) = 0$ are located around the zeros of J_0, $2.4048, 5.5201$ and 8.6537 (displayed with the only four significant digits). They correspond to N01, N02 and N03 in Fig. 1, respectively. Similarly, the third plot in Fig. 2(c) shows that zeros of $d_2(\lambda) = 0$ are located around zeros of J_1, $3.8317, 7.0156$ and 10.1735, corresponding to N11, N12 and N13 in Fig. 1, respectively. From the first plot in Fig. 2(a) for $n = 0$, it can be seen that zeros of $d_0(\lambda) = 0$ except the leftmost one appear at the locations close to zeros of J_1 as in the case of $n = 2$. More generally, it can be shown that zeros of $d_{\pm n,}(\lambda) = 0$ approach zeros of $J_{\pm(n-1)}(a\lambda) = 0$ for $n \geq 0$ as $\varepsilon \to 0$, in other words, the resonance frequency of order $n(\geq 0)$ appears near an eigenvalue of order $n - 1$ of the cloaked region. To do this, using the identity of Bessel functions, $\mathcal{C}_{-n} = (-1)^n \mathcal{C}_n$ for $\mathcal{C}_n = J_n$ or H_n^1, it suffices to prove the convergence of zeros of $d_{n,\varepsilon}(\lambda) = 0$ to those of $J_{n-1}(a\lambda) = 0$ for $n \geq 0$. The identity of Bessel functions $\mathcal{C}_n'(z) = \mathcal{C}_{n-1}(z) - n/z\mathcal{C}_n(z)$ [19] transforms $d_{n,\varepsilon}(\lambda) = 0$ to

$$D_{n,\varepsilon}(\lambda) \equiv \frac{aJ_{n-1}(a\lambda)}{J_n(a\lambda)} - \frac{\varepsilon H_{n-1}^1(\varepsilon\lambda)}{H_n^1(\varepsilon\lambda)} = 0. \tag{13}$$

Now, since $\varepsilon H_{n-1}^1(\varepsilon\lambda)/H_n^1(\varepsilon\lambda) \to 0$ as $\varepsilon \to 0$ [19], $D_{n,\varepsilon}(\lambda)$ is a small analytic perturbation of the function $aJ_{n-1}(a\lambda)/J_n(a\lambda)$ for small ε. Thus the perturbation theory proves the convergence of zeros of $d_{n,\varepsilon}(\lambda) = 0$ to those of $J_{n-1}(a\lambda) = 0$ as $\varepsilon \to 0$.

The convergence behavior of the first three resonance eigenvalues for $n = 0, 1, 2$ as a function of ε is illustrated in Fig. 3. It shows that the convergence rate for $n = 0$ is slower than that for other order $n \neq 0$ since the Hankel function of the zeroth order has the logarithmic singularity at the origin. From this fact, we can predict the location of resonance frequencies of the imperfect cloaking devices and identify the shape of the corresponding resonance modes. It is worth noting that the eigenvalue of the cloaked region of order 1 is approached by resonance frequencies of two different orders 0 and 2, while the eigenvalues of order $n \neq 1$ is approached by resonance frequencies only of order $n-1$. This unique phenomenon associated with the eigenvalue of the cloaked region of order 1 can be found as resonance peaks and dips N11, N12 and N13 in the TSCS spectrum of Fig. 1 in contrast to single peaks for other eigenvalues.

Now, we conduct numerical calculations for resonance modes with $a = 1$ when a plane wave of the unit amplitude travels from the left to the right along the x-direction. The snapshots of different resonance modes N02, N12A and N12B in Fig. 1 of the imperfect cloaking with $\varepsilon = 0.0001$ are presented in Fig. 4. The left of the plots illustrates total fields in the region containing the cloaking device. It is observed that when the wavenumber k is set to be a resonance frequency, transmitted fields into the concealed region are highly excited as already reported in Ref. [13]. In order to examine the cloaking effect for scattered fields, the exterior pressure fields outside of the disc $B_{1.02}$ of radius 1.02 are also provided in the right of the plots.

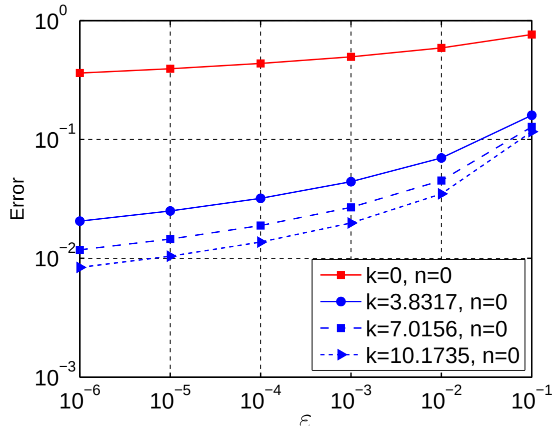

(a)$n = 0$

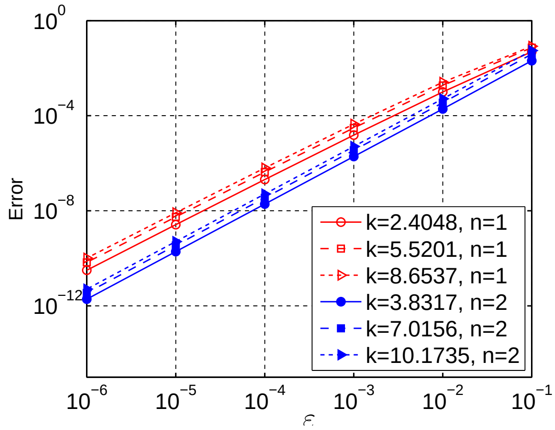

(b)$n = 1, 2$

FIG. 3. Errors of the resonance eigenvalues as functions of ε for $n = 0, 1, 2$ when $a = 1$

For the first case, we choose $k = 5.5201$ corresponding to the N02 mode, which is located near a zero of J_0. Since the denominator d_1 of the first order coefficients nearly vanishes in the vicinity of k, the first order cylindrical wave term is significantly resonated and consequently a dipole mode appear near the zero of J_0 as depicted in Fig. 4(b).

For the second case, we investigate a resonance peak N12B ($k = 7.0340$) and dip N12A ($k = 7.0156$). The snapshots of total pressure fields are provided in Fig. 4

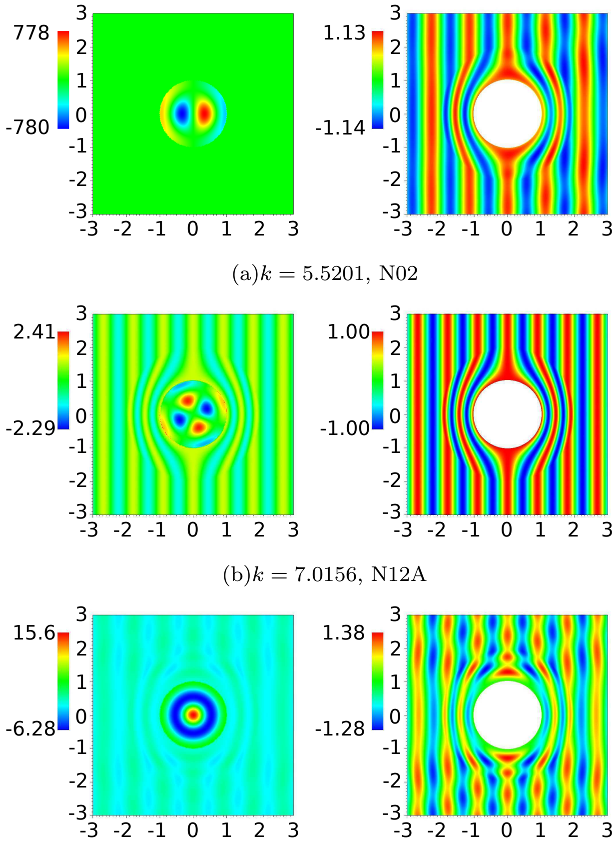

(a)$k = 5.5201$, N02

(b)$k = 7.0156$, N12A

(c)$k = 7.0340$, N12B

FIG. 4. Snapshots of acoustic pressure fields of the imperfect cloaking with $\varepsilon = 0.0001$: total pressure fields on the whole region (left) and outside of the disc $B_{1.02}$ of radius 1.02 (right)

(c) and (d). The observation obtained from the left snapshots of Fig. 4 (c) and (d) is that almost perfect cloaking can be achieved for the N12A mode while the performance of the cloaking for the N12B mode is noticeably weakened, which is consistent with the fact that the N12A mode arises at the dip of TSCS and the N12B mode does at the peak. The same computational result can be found in Ref. [13]. Next, we see that the N12A mode exhibits an excited quadrupole resonance and the N12B mode does a monopole resonance. This fact can be explained as follows. We first note that the wavenumber $k_0 = 7.0156$ (a zero of J_1 displayed with only four significant digits) is approached by two zeros of d_2 and d_0 as $\varepsilon \to 0$. The zero of d_2 converges to k_0 much faster than the zero of d_0 as indicated in Fig. 3, which implies that the second order cylindrical wave term is excited at the frequency of N12A showing a quadrupole resonance and the zeroth order cylindrical wave term is enhanced at the frequency of N12B resulting in a monopole resonance. It is worthy of remark that monopole and quadrupole resonance modes always appear near each other in the TSCS spectrum.

In conclusion, we have studied the resonance phenomenon arising from the imperfect cloaking based on a small perturbation of the transformation acoustics. It is verified that resonance frequencies are close to Dirichlet eigenvalues of the concealed region when the perturbation parameter ε is sufficiently small. In particular, the n-th order cylindrical wave term is resonantly excited at frequencies near zeros of $J_{n-1}(a\lambda) = 0$. Also, the computational results demonstrate that resonance modes are almost trapped near the cloaked region. This theory enables us to predict not only the location of resonance frequencies but also the shape of corresponding resonance modes. We expect this theory may be used to develop a cloaking structure that can avoid resonance phenomena and improve the cloaking effect.

[1] Greenleaf A, Lassas M and Uhlmann G 2003 Comm. Pure Appl. Math. **56** 328
[2] Greenleaf A, Lassas M and Uhlmann G 2003 Math. Res. Lett. **10** 685
[3] Pendry J B, Schurig D and Smith D R 2006 Science **312** 1780
[4] Chen H and Chan C T 2007 Appl. Phys. Lett. **91** 183518
[5] Cummer S A and Schurig D 2007 New J. Phys. **9** 45
[6] Greenleaf A, Kurylev Y, Lassas M and Uhlmann G 2007 Comm. Math. Phys. **275** 749
[7] Norris A N 2008 Proc. R. Soc. A **464** 2411
[8] Torrent D and Sánchez-Dehesa J 2008 New J. Phys. **10** 063015
[9] Chen H and Chan C T 2010 J. Phys. D: Appl. Phys. **43** 113001
[10] Schurig D, Mock J J, Justice B J, Cummer S A, Pendry J B, Starr A F and Smith D R 2006 Science **314** 977
[11] Greenleaf A, Kurylev Y, Lassas M and Uhlmann G 2008 New J. Phys. **10** 115024
[12] Ruan Z, Yan M, Neff C W and Qiu M 2007 Phys. Rev. Lett. **99** 113903
[13] Cheng Y and Liu X J 2009 Chin. Phys. Lett. **26** 014301
[14] Kundtz N, Gaultney D and Smith D R 2010 New J. Phys. **12** 043039
[15] Cheng Y and Liu X J 2008 Appl. Phys. Lett. **93** 071903
[16] Cai L W and Sánchez-Dehesa J 2007 New J. Phys. **9** 450
[17] Cheng Y, Yang F, Xu J Y and Liu X J 2008 Appl. Phys. Lett. **92** 151913
[18] Chen H, Liang Z, Yao P, Jiang X, Ma H and Chan C T 2007 Phys. Rev. B **76** 241104
[19] Abramowitz M and Stegun I A 1964 Handbook of mathematical functions with formulas, graphs, and mathematical tables (New York: Dover) chap 9 p355